RSC Advances

ROYAL SOCIETY OF CHEMISTRY

www.rsc.org/advances

Electrochemical Sensing of Dopamine at the Surface of Dopamine Grafted Graphene Oxide / Poly (Methylene Blue) Composite modified electrode

Demudu Babu Gorle and Manickam Anbu Kulandainathan*

Electrochemical Process Engineering Division, CSIR-Central Electrochemical Research Institute, Karaikudi, India

* Email: manbu123@gmail.com

ABSTRACT

Simultaneous electrochemical reduction of graphene oxide (GO) and oxidative polymerization of methylene blue yielding polymer composite on glassy carbon electrode surface is demonstrated. The stability of the reduced graphene oxide (ERG)/poly (methylene blue) (PMB) composite in buffer solution is also studied in detail. Interestingly, methylene blue initially forms a radical cation, which donates an electron to GO, further GO undergoes reduction and during subsequent cycles, it forms the polymer composite through covalent interactions between simultaneously reduced GO and oxidized methylene blue. The formation of polymer composite is characterized through Electrochemical Impedance Spectroscopy, Laser Raman Spectroscopy, SEM and UV-Visible absorption studies. Dopamine is a neurotransmitter having primary amine and phenolic functional groups. Electro grafting of dopamine onto ERG/PMB composite modified electrode is carried out and is evaluated by FT-IR, XPS studies and the electrochemical stability of the grafted dopamine is demonstrated through CV studies. The Differential pulse voltammetry studies reveal that the modified electrode shows high selectivity and sensitivity towards the detection of dopamine in the presence of Ascorbic acid (AA) and Uric acid (UA) with a detection limit of 1.03×10^{-6} mol L^{-1} from calibration curve with linear range 0.96×10^{-6} mol L^{-1} to 7.68×10^{-6} mol L^{-1}. Hence, this dopamine grafted on polymer composite modified electrode provides an attractive platform for selective sensing of dopamine in the presence of interferents.

Keywords: Electro grafting, Graphene Oxide, Methylene Blue, Polymerization, Catalytic activity.

1. INTRODUCTION

Graphene,[1] is a single layer of graphite consisting of sp^2 carbon atoms packed in 2D honeycomb lattice, which has been studied and used for remarkable applications such as polymer Nano composites,[2,3] energy,[4] sensors,[5] biomedical,[6] liquid crystal devices,[7] field effect transistors,[8] flexible materials[9] and mechanical resonators[10] due to its unique properties[11,12,13,14,15,16] which includes mechanical, electrical, thermal, electronic and optical properties. The hydrophobic[17] nature of graphene tends to form irreversible agglomeration in aqueous solution due to the strong π-π stacking interaction. This explains the poor solubility of graphene in polymer matrices, which limits its applications**.** Graphene can be synthesized by both top-down and bottom-up approaches, which includes Chemical Vapor Deposition(CVD), micromechanical cleavage, epitaxial growth on metal surface and reduction of graphite oxide and GO.[18,19] Large scale synthesis of graphene has been carried out through chemical, thermal and electrochemical reduction methods.[20,21] Among these methods, electrochemical reduction is one of the finest routes because it is a simple, time saving and eco-friendly process and through this method one can avoid the usage of environmentally harmful reductants.

Electro polymerization is an effective method for the synthesis of polymeric thin films of dye,[22] heterocyclic compounds[23] etc. Methylene blue (MB) is a cationic water-soluble phenothiazine dye. Many research groups have prepared graphene/MB polymer composite by electrochemical method and it was used as a catalyst in biological applications. Christopher et al**.,** prepared phenazine polymers and used in biosensors.[24] Wei Sun et al**.,** fabricated poly (MB) functionalized graphene modified carbon ionic liquid electrode for dopamine detection.[25] Alanyalioglu et al**.,** synthesized poly (MB)/graphene Nanocomposite thin

films for oxidation of nitrite.[26] Wojtoniszak et al**.,** functionalized graphene oxide with MB and used as performer in singlet oxygen generation.[27]

The term electro grafting refers to electrochemical reaction between the organic molecules and solid conducting materials. Further, it was extended to reactions involving an electron transfer between the reagent and substrate in the modified electrode surfaces. Electro grafting applies to many functional groups like amines, carboxylates, alcohols, Grignard reagents, vinylics, diazonium salts, ammonium salts, phosphonium salts and sulfonium salts etc.[28,29] Electro grafting is a well-established method for surface modification and used in various applications like sensors, biomolecules, energy storage devices and industrial applications.[30] The reactive pathway in electro grafting can either be oxidative or reductive depending upon the redox behavior of molecules.

In this communication, initially we prepared ERG/PMB composite electrochemically and demonstrated the electro grafting of dopamine on prepared polymer composite surface, which is expected to enhance the electron transfer kinetics of the modified surface. Electro grafting of dopamine follows oxidative method through amine linkages.[31] The grafting of dopamine on to modified electrode was explained using Fourier transformed infrared spectroscopy (FTIR) and X-ray photoelectron spectroscopy (XPS) analysis. Dopamine grafted modified electrode is a good catalyst at sensing of dopamine through the "like recognizes like"[32] principle, which was explained from CV studies and interference of dopamine with UA and AA was explained through DPV studies. **Scheme 1** depicts the reaction pathway of total system as explained in the later sections.

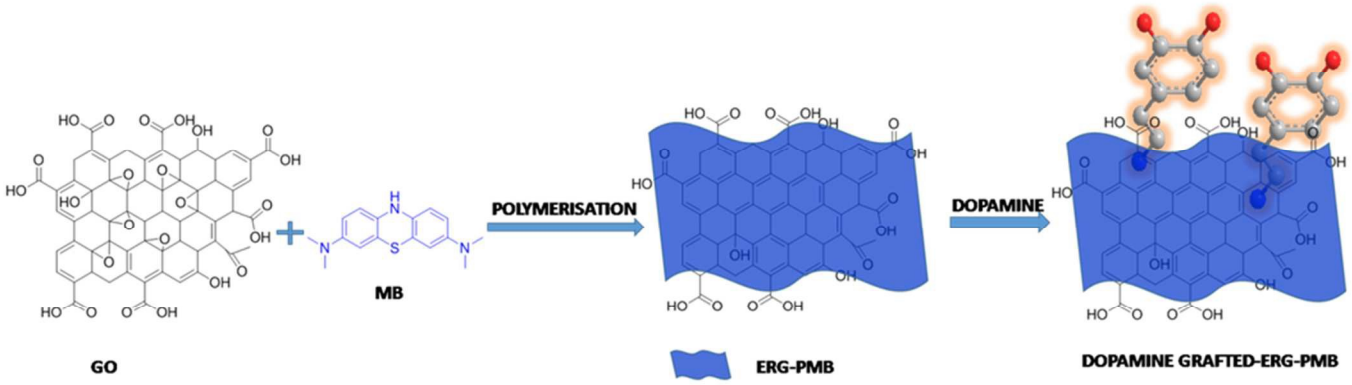

Scheme 1. General Reaction pathway of electrochemical polymerization and grafting of dopamine.

2. EXPERIMENTAL SECTION

Materials

Graphite powder(Alfa Aesar), Sodium Nitrate (Sigma Aldrich), Sulfiric acid (AR,Ranbaxy), Potassium permanganate (Sigma Aldrich), 30% Hydrogen peroxide (Alfa Aesar), Monopotassium Dihydrogen Phosphate and Dipotassium Mono hydrogen Phosphate(Extrapure AR,SRL), Methylene Blue (high purity,AlfaAesar), Potassium Chloride(Sigma Aldrich), Potassium Ferri and Ferro cyanide(SRL), Dopamine hydrochloride, Ascorbic acid and Uric acid (98.5%, Alfa Aesar) were used in the experiments as received. In all the experiments, distilled water with conductivity of 36 µS cm^{-1} was used for preparing the solutions.

Preparation of GO:

Graphite oxide was prepared from graphite powder following the procedure adopted in Hummers method.[33] 5 g of graphite powder (99.9%) was added to 115 mL of Concentrated Sulfuric acid containing 2.5 g of sodium nitrate in 500 ml beaker under vigorous stirring. Once addition was completed, it was kept in an ice-bath and the temperature was maintained below 10 $^{\circ}$C. At this temperature, 15 g of potassium

permanganate was added to the solution mixture carefully to prevent the increase of solution temperature beyond 20 °C. The solution was removed from the ice-bath and kept for 30 min at temperature 30-35 °C. A brownish yellow color paste was formed at the end of 20 min by the elimination of gas. After 30 min, 230 mL of water was added slowly and the temperature was raised to 90 °C and maintained for 15 min. Later, this was further diluted with 700 mL of warm water and eventually removal of residuals were carried out by the addition of 30% hydrogen peroxide. Finally, brown yellow graphite oxide solid was obtained by filtration followed by centrifugation and was dried at 60 °C for 24 h.

GO was prepared by sonicating the graphite oxide powder in water[34] for this, graphite oxide (2 mg/ml) was dissolved in distilled water and sonicated approximately for 2 h, which finally gave dark yellow color solution. At the end, this was centrifuged, filtered, washed thoroughly with distilled water and dried at 100 °C for 8 h.

Instrumentation

Laser Raman analysis of Fluorine doped Tin Oxide (FTO) coated substrate was carried out by Renishaw Invia Raman Microscope with He-Ne Laser 633 nm (Renishaw, U.K.), The morphology of the sample coated on the FTO plate was studied by S-3000H SEM with 30-300000 x magnification (Hitachi, Japan). The absorption of MB solution was studied using UV-VIS-NIR Double Beam Spectrophotometer of Cary 500 Scan Model and FTIR Spectrum of the sample was analyzed through BRUKER TENSOR 27 FT-IR Spectrometer (Bruker Optik GmbH, Germany). The chemical composition of the surface modified by electrochemical polymerization and electro oxidative grafting of dopamine on to the FTO coated electrode was studied by XPS technique (Multilab 2000, Thermo scientific, U.K). An Al Kα radiation was used as X-ray source with pass energy 20 eV to record the spectrum with a scan range of 0-1150 eV binding energy and pressure was about 3 x 10^{-8} Torr. The binding energies of all atoms in the modified surface were referenced

by the 1s hydrocarbon peak at 286.4 eV and the XPS spectra was fitted with Shirley-type background by the XPS PEAK 4.1 software with Gaussian-Lorentzien 60%/40 % technique.

Cyclic Voltammetry, Electrochemical Impedance spectroscopy and Differential Pulse Voltammetry (DPV) studies were carried out using BAS-IM6 (Zahner Messsysteme, Germany) instrument under three-electrode cell system. Glassy carbon electrode with 3mm diameter was used as a working electrode. SCE electrode and Platinum wire were used as a reference and auxiliary electrodes, respectively. Prior to use, GC electrode was cleaned using alumina paste (0.05 μ) on emery polishing paper (2/0) for 3 min. Further it was sonicated, washed thoroughly with water and ethanol. Finally, it was dried using nitrogen gas. Before each experiment, the electrolyte was deoxygenated by purging with nitrogen gas for 20 min. All experiments were done at room temperature.

3. RESULTS AND DISCUSSION

Electrochemical preparation of ERG/PMB composite:

ERG/PMB composite was prepared by electrochemical polymerization method.[35] In this method, drop-casted GO coated GC surface was used as a working electrode and the procedure is as follows. Herein, 10 μL of GO solution was coated on the surface of ultrasonically cleaned glassy carbon electrode and dried at room temperature for 4 h. The electrolytic solution was prepared with 0.026 mM MB in 0.1M phosphate buffer solution with pH 7.4. Electrochemical polymerization was carried out by potential cycling between -1.5 to 1.3 V vs. SCE at a scan rate of 50 mV s^{-1}. Figure 1(A) shows the cyclic voltammogram of electrochemically reduced ERG/PMB composite prepared via electrochemical polymerization method. It can be demonstrated that the position of oxidation peak and the reduction peak moves towards higher values from the 1st cycle to 20th cycle.

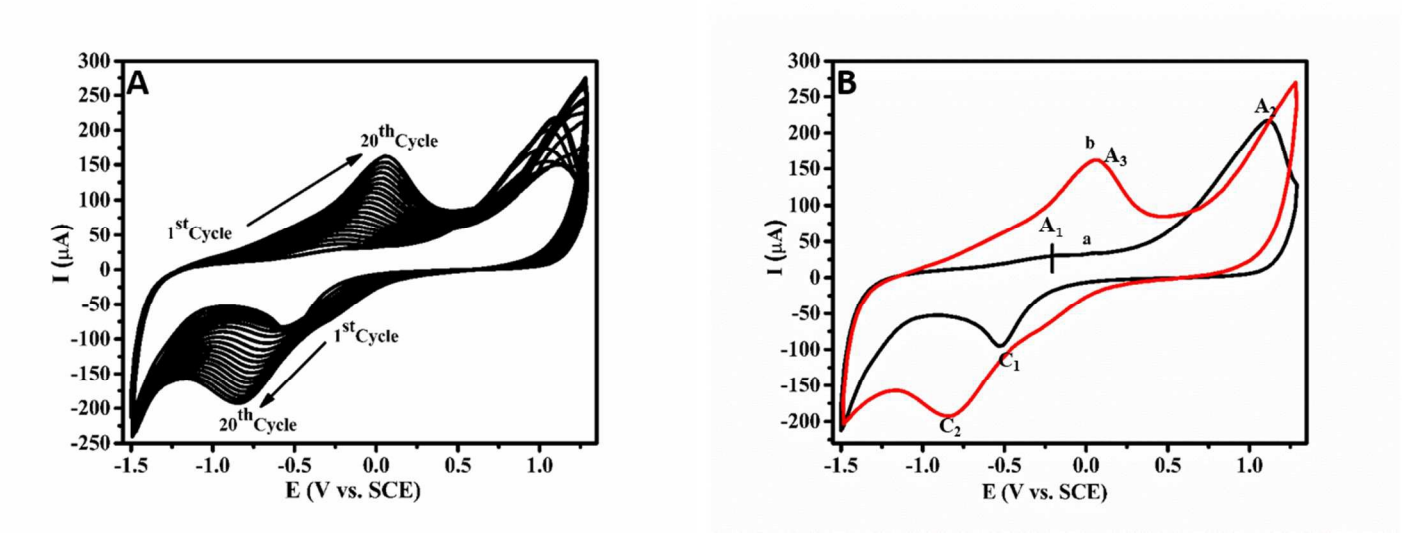

Figure 1. (A) Electrochemical polymerization of GO/MB modified electrode at 50 mV s^{-1} for 20 cycles (B) (a) 1st, (b) 20th cycles of electrochemical polymerization.

Figure 1(B) shows 1st and 20th cycles of electrochemical polymerization. During the 1st cycle, a well-defined reduction and oxidation peaks were observed at -0.53 (C_1) and -0.19 V (A_1) vs. SCE respectively. This pair of redox peak corresponding to the reduction of GO and oxidation of MB at the interface.[26] The current rapidly rises more positive potential nearly at 1.12 V (A_2) vs. SCE is assigned to formation of MB radical cation.[36] After this potential value, MB under goes electrochemical polymerization through the formation of radical cations.[37] Interestingly, the reduction current of GO at -1.48 V vs. SCE decreases very less from 1st to 20th cycles, which suggest that the electrochemical reduction of GO was completed.[38] In 20th cycle, another pair of redox peaks were formed at -0.84 (C_2) and 0.05 (A_3) V vs. SCE with increasing the current with cycles, which depends amount of GO reduction and formation of PMB film on the modified electrode surface.[37] From this, we can clearly explain the simultaneous redox behavior of MB and GO forming ERG/PMB composite and this behavior depends upon the concentration of MB (Figure S1, S2 and S3 as Supporting Information). Similarly poly (MB) modified GC electrode as well as electrochemically reduced GO modified GC electrode were prepared by the same procedure (Figure S4 and S5 as Supporting

Information). The expected mechanism for the formation of ERG/PMB composite by electrochemical process is shown as Scheme S1 (Supporting Information).

Figure S6(Supporting Information) shows the cyclic voltammogram of the bare GC, GO and ERG coated GC electrodes in potassium phosphate buffer solution (pH 7.4) at a scan rate of 50 mV s^{-1} between -1.5 to 1.3 V vs. SCE. Accordingly, GO and ERG coated electrodes exhibited one redox couple with an anodic peak at 0.5 V and a cathodic peak at -1.25 V vs. SCE, whereas the bare GC electrode showed a featureless voltammogram. The cathodic current of GO was -0.406 mA at -1.5 V, which is found to be decreasing with ERG, thus it demonstrates the subsequent reduction of GO from 1st to 20 cycles. GO started reducing to irreversible ERG and after almost 20 cycles, the stability of the cathodic current shows complete reduction of GO. High anodic current was observed with GO may be due to the over oxidation of chemical impurities present in GO. After coating with GO and its reductant on to the surface of the GC electrode, it shows the high current which suggests that the GO and ERG provide the conduction path for electron transfer at electrode/ electrolyte interface and used in the electrochemical catalytic reactions as a catalyst.[39] The change in the position of the redox couple towards high redox potential value and the high capacitive behavior of the modified electrode explains the improvement in the non-Faradaic current of ERG due to the increase of conductive surface area by the electrochemical reduction.[40]

The surface area of the polymer film formed on the GO coated GC electrode can be calculated from the surface coverage concentration of PMB.[35,41] The value of charge involved in the polymerization can be calculated from the peak area appeared in the cyclic voltammogram using the following formula;

$$\Gamma = Q / (nFA)$$

Where A is the area of the GCE (0.07065 cm^2), F is Faraday constant (96485.34 C mol^{-1}), Γ is the surface coverage concentration and n is the number of electrons involved in the electrochemical polymerization of

MB (n = 2). The value of charge (Q) can be calculated from the integration of peak area between -0.37 to 0.48 V vs. SCE at scan rate 50 mV s^{-1} is 8.314 μC. Using the above values, Γ value calculated for polymer film to be $6.13x10^{-10}$ mole cm^{-2}. Finally, Γ value demonstrates a good surface coverage of PMB film on the modified electrode surface. From this, we clearly notice that 10 μL of GO was covered by 6.13×10^{-10} mol cm^{-2} of MB.

The electrochemical activity of GO coated GC electrode was characterized by the reaction with MB in buffer solution with pH 7.4 (FigureS7 as Supporting Information). In that, GO modified GC electrode has the redox peaks at -0.53 V and 1.12 V vs. SCE in MB solution, which were present as minor peaks in bare GC as shown in the inset and also shows the high anodic and cathodic current that demonstrates the redox behaviour of MB.

The stability of ERG/PMB composite modified electrode was checked by recording 30 cycles in the same electrolyte solution in the same potential window, which is shown in the Figure S8 (Supporting Information). It is noted that the changes in current are negligible after 30 cycles, which indicates the stability of ERG/PMB composite modified electrode. Based on this result, it is very clear that the formed polymer composite material is highly stable and active and it is suitable catalytic electrode for electrochemical redox reactions.

The formation of PMB, ERG and ERG/PMB composite was verified by Electrochemical impedance spectroscopy (EIS)[24,35] and CV studies (Figure S9 as Supporting Information). Figure 2 shows the impedance behavior of modified electrodes in 2 mM L^{-1} $[Fe(CN)_6]^{3-/4-}$ in 0.1 M KCl solution with an amplitude of 30 mV and frequency ranging from 10^6 Hz to 0.05 Hz. In this, ERG shows semicircle at low frequency region with Rct of about 1.12 kΩ, which makes it difficult for the electron transfer between electrode/electrolyte interface. The semicircle at high frequency region completely disappeared in the case of PMB and

ERG/PMB composite modified electrode due to the porosity formed during the formation of the film, indicating that the electron transfer can be fast and diffusion-controlled.

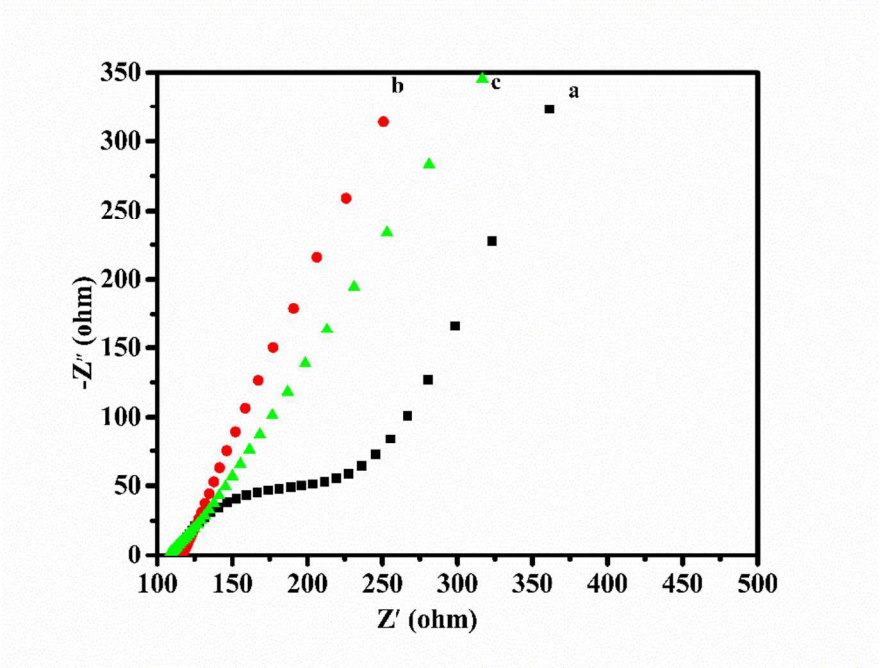

Figure 2. Electrochemical impedance spectroscopy of (a) ERG, (b) PMB and (c) ERG/PMB composite modified electrode in 0.1 M KCl solution containing (1:1) 2 mM L^{-1} $[Fe(CN)_6]^{-3/-4}$.

Raman spectrum revealed the polymerization of MB, Reduction of GO by electrochemical method and formation of ERG/PMB composite.[35,42] The spectrum was shown as Figure 3(A). In the Raman spectrum, D and G bands of ERG formed at 1346 cm^{-1} and 1604 cm^{-1} with approximately the same intensity indicates the presence of both sp^3 and sp^2 carbons with equal number which denotes the reduction of GO. Raman spectrum of PMB forms the peaks at 1037 cm^{-1}, 1161 cm^{-1}, 1304 cm^{-1}, 1332 cm^{-1}, 1395 cm^{-1}, 1433cm^{-1}, 1477 cm^{-1}, 1501 cm^{-1} and 1624 cm^{-1}.The band at 1037cm^{-1} relates to strong C-S aromatic stretching frequency in MB and 1395 cm^{-1}, 1433 cm^{-1}relates to bending vibration modes of N-CH_3 group due to polymerization. The peak at 1624 cm^{-1} was attributed to C=C stretching frequency in aromatic ring. The

peaks of both PMB and ERG are observed in the Raman spectrum of ERG/PMB composite with high intensity which confirms the both polymerization and reduction of MB and GO.

The formation of product was further confirmed by SEM images.[43,44] Figure 3(B), (**a)** showed clear thin layer type structure with small crystals of MB which were present on the layer of the GO shown by the circle in the image (**c**). Image (**b)** shows the clear layered structure of ERG coated on the FTO plate. This confirms the polymerization of MB over the surface of GO by electrochemical method.

The consumption in concentration of MB during the electrochemical polymerization was demonstrated by UV-Visible absorption spectroscopy (Figure S10 as Supporting Information) as shown in the Figure 3(C) and it was noted before and after Cyclic Voltammetry of same solution. In this spectrum, two main absorption bands formed at 659 cm^{-1} and 612 cm^{-1} correspond to MB and MB dimer in solution. According to Beer's Law in UV-Visible Absorption Spectroscopy, absorption is directly proportional to concentration of the solution. The figure clearly shows that the decrease in the absorption intensity during the reaction indicates the decrease in concentration of MB. The difference in concentration of MB after 20 cycles is corresponds to MB reacted with GO during the polymerization.[27,45]

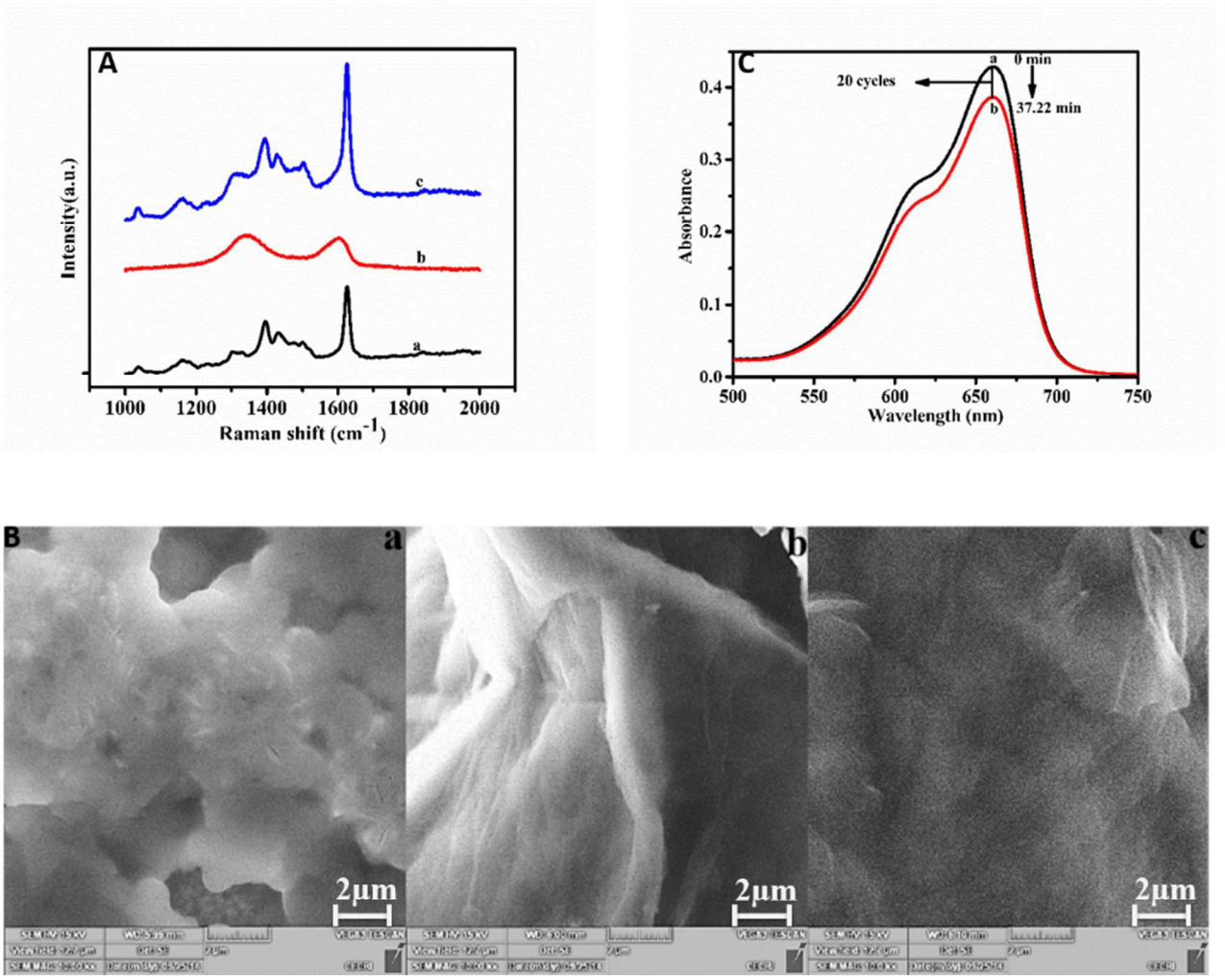

Figure 3. (A) Raman spectrum of (a) PMB, (b) ERG and (c) ERG/PMB composite, (B) SEM images of (a) PMB, (b) ERG and (c) ERG/PMB composite and (C) UV-Visible absorption spectrum of MB solution (a) before Potential Cycling and (b) after Potential Cycling.

Electro grafting of dopamine on the ERG/PMB composite modified electrode: Figure 4(A) shows the CV curves of the 1×10^{-3} mol L^{-1} dopamine in 0.1M Sulfuric acid as electrolyte. The electro grafting of dopamine was performed by 10 successive cycles in the potential range of -0.2 to 1.6 V vs. SCE with scan rate of 50 mV s^{-1}.

In the cyclic voltammogram, an anodic peak with high oxidation current was formed at 0.384 V vs. SCE indicating the oxidation of primary amine to amine radical in dopamine which is strongly attached to ERG/PMB composite material due to its activity on electrode surface by chemical bond.[31] After first cycle, a constant redox peak was formed between the potential region of 0.3 to 0.4 V vs. SCE with ΔE = 56 mV which indicates the attachment of incoming dopamine molecules on the surface of the grafted dopamine molecule shown in the Figure 4(A). The Figure 4(B) shows, the modified electrode has a higher oxidation current in comparison to bare GC electrode in the presence of dopamine (Figure S11 as Supporting Information), which demonstrates the activity of coated material.

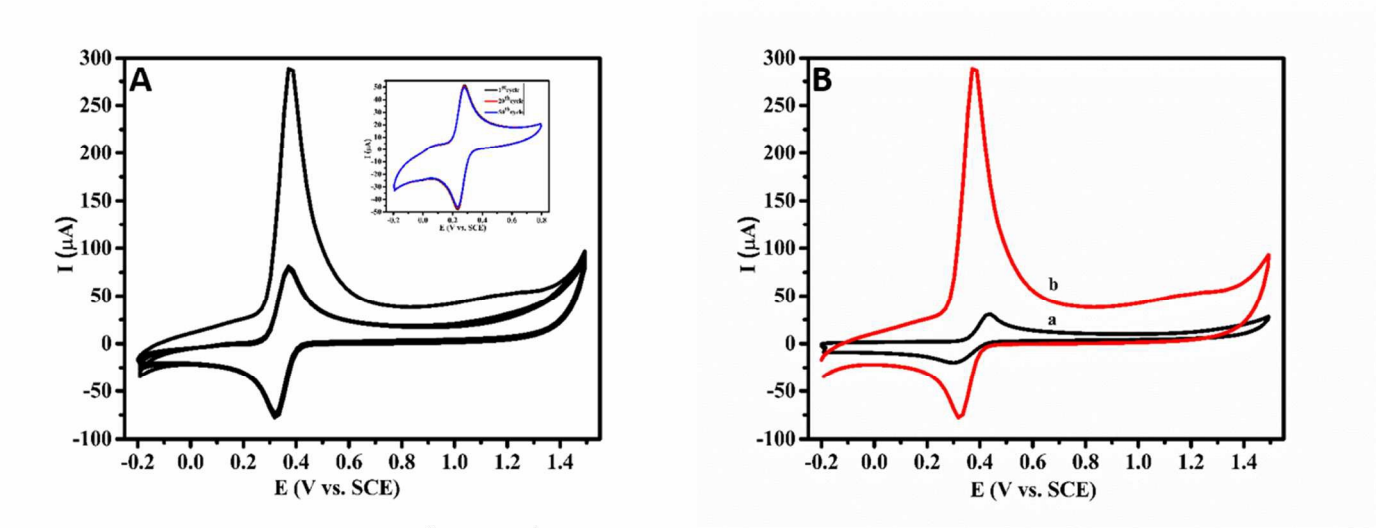

Figure 4. (A) Grafting of 1 × 10^{-3} mol L^{-1} dopamine in 0.1M H_2SO_4 solution for 10 successive cycles at scan rate 50 mV s^{-1}, (Inset) 1st, 20th, 50th cycles of grafted dopamine ERG/PMB composite modified electrode and (B)1 × 10^{-3} mol L^{-1} dopamine with (a) GC and(b) ERG/PMB composite modified electrode. Scan rate 50 mV s^{-1}.

Finally, the electrode was thoroughly washed with water and the grafting of dopamine on modified electrode was studied by cyclic voltammetry. After washing, the ERG/PMB composite modified electrode shows high oxidation current than the bare GC electrode (Figure S12 as Information).The CV shows potential of redox peak at ΔE = 51 mV which is responsible for the redox behavior of dopamine. This

reaction is a one electron transfer reaction which leads to the immobilization of dopamine onto the modified electrode surface. Hence, one of the phenolic groups in the dopamine should undergo oxidation which is explained by the FT-IR and XPS analysis later. Furthermore, the formation of film was confirmed by the sensing of dopamine due to high electron transfer between incoming molecule and active catalytic material through the film.

Figure 4(A) inset shows the 1st, 20th and 50th cycles of dopamine grafted onto the modified electrode surface for 50 cycles in acidic solution. The stability of this material is very high due to its less current variation from the 1st to 50th cycle because all cyclic voltammograms are similar and no change in the potential difference and current of redox peaks. The polymer composite material is highly efficient for the grafting of dopamine.

The grafting and high stability of dopamine film was investigated by the scan rate effect of cyclic voltammetry in the potential range from -0.2 to 0.8 V vs. SCE as shown in the Figure S13(A) (Supporting Information). In this, a well defined redox peak appears and shows increase in the peak current with scan rates . The Figure S13(B) (Supporting Information), the linear relationship between peak current versus square root of scan rate. In this, the slope of the I_{pa} curve (6.11 μA) is greater than the slope of I_{pc} (-5.38 μA) vs $\nu^{1/2}$ means, the process of grafting is oxidation with high electron transfer and it is confirmed by the negligible increase in potential difference in peak separation with scan rate. All these experiments clealy explains that the grafting of dopamine is a surface controlled process on the modified electrode surface.

Surface chemical composition investigation: Surface chemical composition of ERG/PMB modified electrode and electrografted dopamine modified ERG/PMB modified electrode was analyzed by XPS, dopamine and Grafted dopamine was studied by FT-IR Spectroscopy.[31] For these studies, the FTO coated

electrode was used as working electrode which will not change the electrochemical behavior of the coated material instead of GC electrode and followed the same procedure described above.

Figure S14 (Supporting Information) compares the FT-IR Spectrum of both dopamine and grafted dopamine.The intensity and vibrational frequencies of grafted dopamine are found to decrease, which implies the strong attachment of dopamine on the modified electrode surface.[46,47] The evidence of the grafting was explained by the various vibrational bands.The broad absorbance band with high intensity at 3442 cm^{-1} corresponds to N-H stretching in 1°amines or O-H stretching in alcohols.The band at 2960 $cm^{-1}$was attributed to C-H stretching in alkanes and 1736 cm^{-1} corresponds to C=O stretching in carbonyl compounds which confirms the grafting of dopamine on the electrode surface through oxidation. This band disappeared in case of pure dopamine.The IR peaks at 1604 cm^{-1} and 1613 cm^{-1} is expected to be of C=C stretching in aromatics and N-H bending in 1° amines.The observations of these peaks in dopamine spectrum with higher vibration values describes the oxidative grafting of dopamine with modified electrode by electrochemical method.

The surface chemical composition of ERG/PMB modified electrode was analyzed by the XPS spectrum before and after grafting of dopamine and it is a surface sensitive technique.The XPS survey spectrum of C 1s, N 1s, O 1s and S 2p elements are shown in Figure 5. According to XPS spectrum survey, the same elements are present before and after grafting of dopamine. In Figure 5 (A), The deconvolution of C 1s spectra demonstrates the following binding energy values, i.e. 284.48 eV ~ C = C or sp^2 and C-C or sp^3 and C-H because the peaks are not identified separately due to resolution of XPS spectrometer and 285.25 eV ~ C-N and 286.95 eV ~ C-O with 13.92 %.[48] After grafting of dopamine (Figure 5 (B)), the new peak was observed at 288.52 eV with 7.75 % which may be identified as C = O corresponding to the oxidation of phenolic group in grafted dopamine due to incoming dopamine molecules and also 284.56 eV ~ C can be identified as a phenolic group[49] with high atomic percentage (53.42 %). The spectrum of O 1s was

observed in both cases at 530.72 eV and 531.17 eV corresponding to C = O group after grafting based on the literature reports.[50,51] The N 1s region fitted as two peaks at 398.76 eV and 401.29 eV with high atomic percentege demonstrates a primary and tertiary amine groups of dopamine as well as MB. This indicates that the high number of dopamine might be undergoes to grafting.[46] S 2p region is fitted with two peaks assigned as SO and SO_3 groups with atomic percentage 87.78 % and 12.21 % respectively. Interestingly, after the grafting of dopamine, the atomic percentage of former (46.48 %) was less than the later (53.51 %). According to this, the more number of oxygen atoms from incoming molecules of oxidized dopamine might be reacting with sulfur in the Methylene Blue.[52,53]

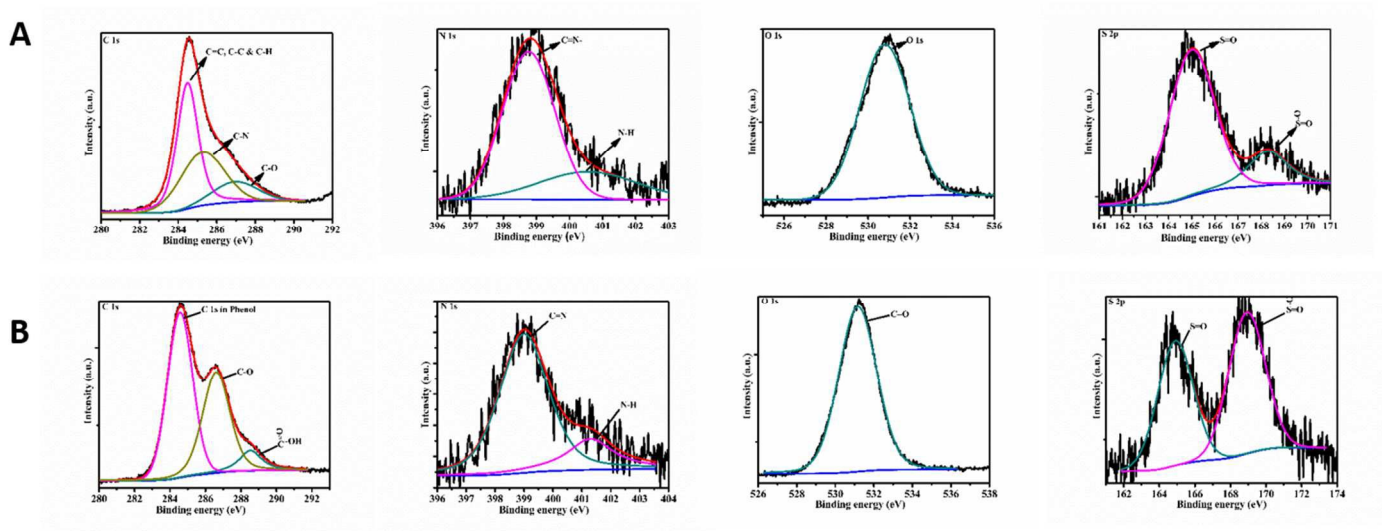

Figure 5. XPS spectra of C 1s, N 1s, O 1s and S 2p of ERG/PMB modified electrode (A) before grafting of dopamine (B) after grafting of dopamine.

Electrocatalytic activity of dopamine grafted ERG/PMB modified electrode towards the Sensitivity of dopamine: Figure 6 shows the electrochemical response of the bare GC, ERG, PMB, ERG/PMB and dopamine grafted ERG/PMB modified GC (A) without dopamine and (B) with 118.5 × 10^{-6} mol L^{-1} dopamine in pH 7.4 Phosphate buffer solution at scan rate 50 mV s^{-1}. In Figure 6 (A), the back ground current of dopamine grafted ERG/PMB modified electrode was high and one redox peak was observed in range of -0.2 to 0.2 V vs. SCE, demonstrates the attachment of dopamine on the surface of the ERG/PMB modified GC electrode. Figure 6 (B) shows the electrocatalytic activity of five electrodes towards the dopamine. In this, the dopamine grafted ERG/PMB modified GC shows the high oxidation current of dopamine between the -0.1 to 0.3 V vs. SCE region than the remaining modified electrodes, which explains that the surface modified with grafted dopamine is highly active

Figure 6 C displays the CV curves of the dopamine grafted ERG/PMB modified GC in pH 7.4 PBS containing different concentrations of dopamine. A well defined redox peak was formed between the region of -0.1 to 0.3 V vs. SCE and peak current was increased with dopamine concentration.It was confirmed by the linear relationship between oxidation peak current and dopamine concentration expressed as Ipa = -8.0894 + 0.59105 C_D (μM) with R^2 = 0.99329, as shown in Figure 6 D.

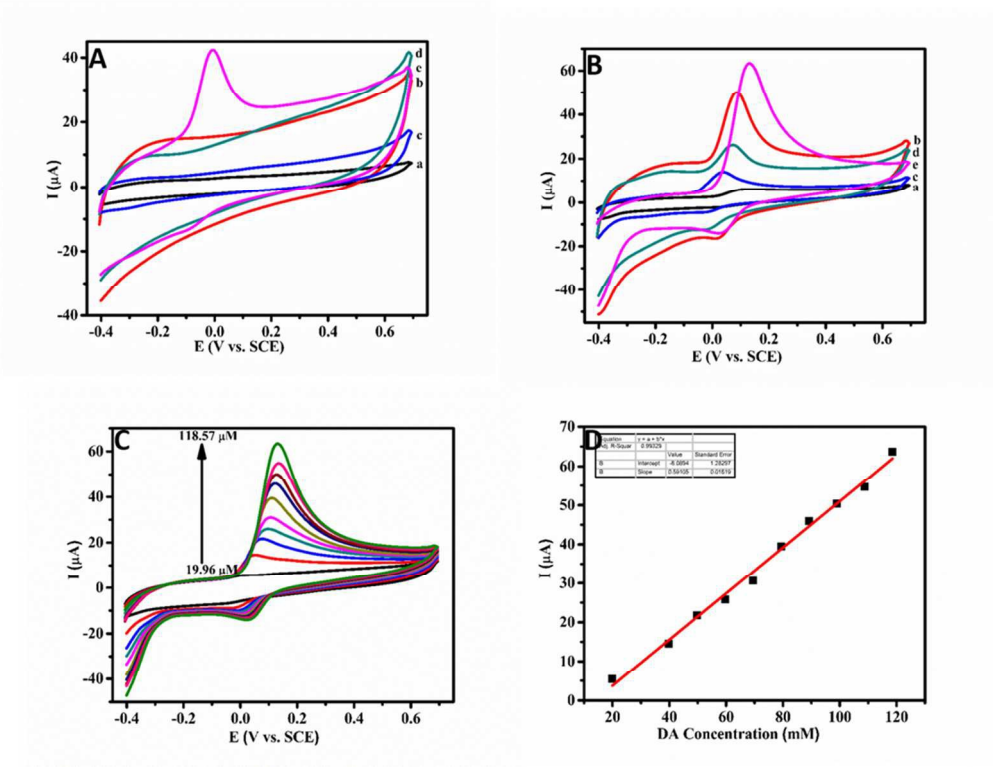

Figure 6. CVs of (a) GC, (b) ERG, (c)PMB (d) ERG/PMB and (e) dopamine grafted ERG/PMB modified GC (A) without dopamine, (B) with 118.57 × 10^{-6} mol L^{-1} dopamine, (C) CVs of 19.96 × 10^{-6} mol L^{-1}, 39.84 × 10^{-6} mol L^{-1}, 49.75 × 10^{-6} mol L^{-1}, 59.64 × 10^{-6} mol L^{-1}, 69.5 5 × 10^{-6} mol L^{-1}, 79.36 × 10^{-6} mol L^{-1}, 89.19 × 10^{-6} mol L^{-1}, 99.00 × 10^{-6} mol L^{-1},108.80 × 10^{-6} mol L^{-1}, 118.57 × 10^{-6} mol L^{-1} dopamine at dopamine grafted ERG/PMB modified GC, Scan rate 50 mV s^{-1}, (D) show the relation between Ipa and concentration of dopamine.

Determination of dopamine at dopamine Grafted ERG/PMB modified electrode:

Dopamine was determined by DPV because of its high resolution and high current sensitivity than CV. Figure 7 A shows DPV responses of dopamine grafted ERG/PMB modified GC toward different concentrations of dopamine from 0.0 × 10^{-6} mol L^{-1} to 47.7 7 × 10^{-6} mol L^{-1} in -0.4 to 0.7 V vs. SCE region. In this ,the anodic peak current of dopamine increases with each addition. Hence, by plotting curve between

peak current and concentration, two different linear curves were observed.[54,55] The first one is corresponds lower concentration range from 5.99 - 11.98 × 10^{-6} mol L^{-1} and second one is corresponds to higher concentration range from 13.98 - 47.77 × 10^{-6} mol L^{-1} with Ipa = 25.43 + 1.75 C_D (R^2 = 0.9958) and 41.76 + 0.39 C_D (R^2 = 0.9962). From this, we explained that the dopamine was oxidized to dopaminoquinone and Leucodopaminochrome due to the high catalytic activity of grafted dopamine on ERG/PMB modified surface. This was also happen in presence of AA and UA. As shown in the Figure 7 B.

Figure 7 C represents the DPV of dopamine at different concentrations where AA and UA concentration kept as constant. Here also,the concentration of dopamine increases in the presence of AA and UA ,there is no change in the peak current of both AA and UA indicates the dismissing of interfere with dopamine. In addition, two different linear relationships between oxidation peak current and concentration from 0.96 × 10^{-6} mol L^{-1} to 42.12 × 10^{-6} mol L^{-1} with two regression coefficients 0.9951 and 0.9918 were shown in Figure 7D. The detection limit for the determination of dopamine in the presence of AA and UA was calculated is 1.03 × 10^{-6} mol L^{-1}. As shown in Table 1, sensing performance of the dopamine grafted ERG/PMB composite modified electrode was compared with that of other electrochemical sensor systems.

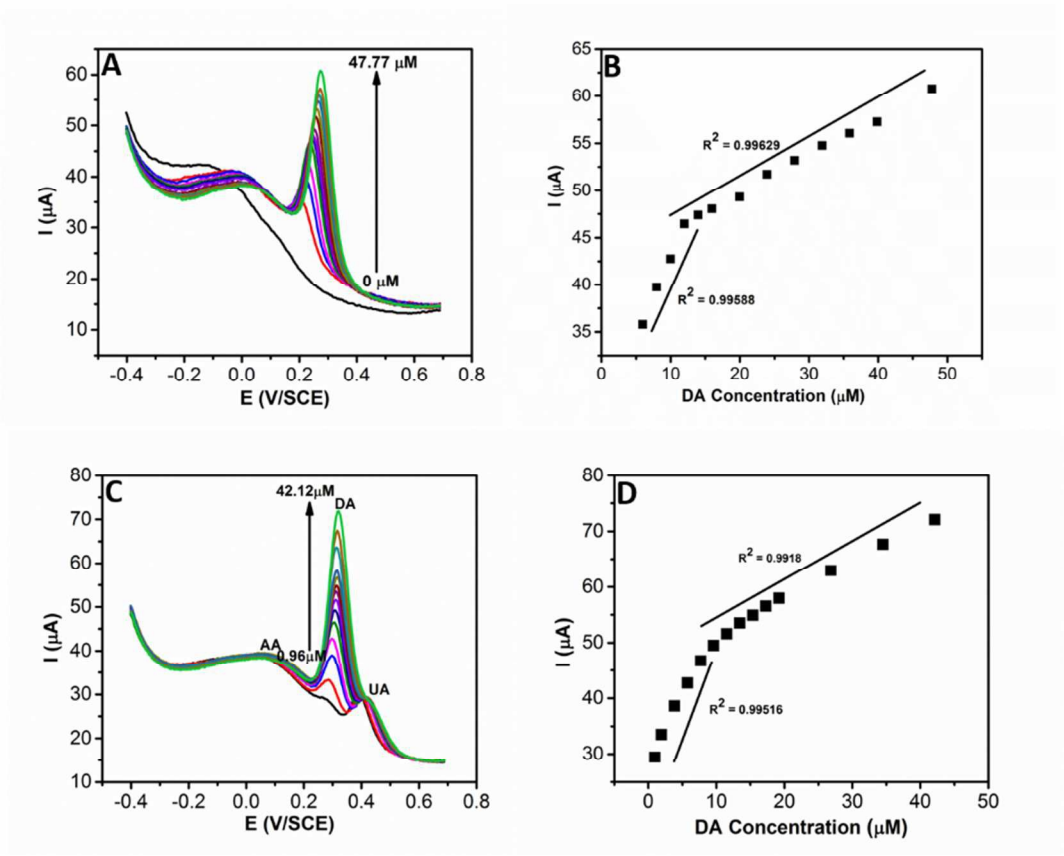

Figure 7. DPVs of (A) 0.00 × 10^{-6} mol L^{-1}, 5.99 × 10^{-6} mol L^{-1} , 7.99 × 10^{-6} mol L^{-1} , 9.99 × 10^{-6} mol L^{-1}, 11.98 × 10^{-6} mol L^{-1}, 13.98 × 10^{-6} mol L^{-1}, 15.98 × 10^{-6} mol L^{-1}, 19.96 × 10^{-6} mol L^{-1}, 23.94 × 10^{-6} mol L^{-1}, 27.92 × 10^{-6} mol L^{-1}, 31.89 × 10^{-6} mol L^{-1}, 35.87 × 10^{-6} mol L^{-1}, 39.84 × 10^{-6} mol L^{-1}, 47.77 × 10^{-6} mol L^{-1} dopamine on dopamine Grafted ERG/PMB Modified GC in 0. 1M PBS (pH 7.4), (B) Relationship between oxidation peak current and concentration of dopamine. (C) 0.96 × 10^{-6} mol L^{-1}, 1.92 × 10^{-6} mol L^{-1}, 3.84 × 10^{-6} mol L^{-1}, 5.76 × 10^{-6} mol L^{-1}, 7.68 × 10^{-6} mol L^{-1}, 9.60 × 10^{-6} mol L^{-1}, 11.52 × 10^{-6} mol L^{-1}, 13.44 × 10^{-6} mol L^{-1}, 15.36 × 10^{-6} mol L^{-1}, 17.27 × 10^{-6} mol L^{-1}, 19.19 × 10^{-6} mol L^{-1}, 26.85 × 10^{-6} mol L^{-1}, 34.49 × 10^{-6} mol L^{-1}, 42.12 × 10^{-6} mol L^{-1} dopamine on dopamine Grafted ERG/PMB Modified GC in the presence of 96.14 × 10^{-6} mol L^{-1} AA and 288.43 × 10^{-6} mol L^{-1} UA in 0.1M PBS (pH 7.4), (D) Relationship between oxidation peak current and concentration of dopamine. Step height : 5 mV; Step width : 1sec; Pulse width : 200 ms; Pulse height : 50 mV and Start ramp : 10 mV sec^{-1}.

Table 1 Comparison of sensing performances of different modified electrodes for the determination of dopamine.

S. No.	Analytical method	Material used	LOD [μM]	Reference no.
1	DPV	PMB-GR/CILE	0.0056	56
2	DPV	$(NG/PEI)_5$/GCE	0.5	57
3	Amperometry	PEDOT/RGO	0.039	58
4	LSV	PDA-RGO/Au	3.211	59
5	DPV	Dopamine grafted ERG/PMB	1.03	This work

4. CONCLUSION

ERG and PMB composite was prepared by Electrochemical Redox method through potential cycling between -1.5 to 1.3 V vs. SCE. The decrease in concentration of MB during cycling was monitored using UV-Visible absorption spectroscopy. The formation of polymer composite was evidenced through Electrochemical Impedance Spectroscopy, Raman and SEM. Electro grafting of dopamine was done on ERG/PMB composite modified electrode surface and redox behavior was explained by potential values. Finally, the grafting of dopamine on the surface of the modified electrode was demonstrated using FT-IR Spectroscopy and XPS analysis. The catalytic activity of the grafted dopamine was higher than the other modified electrodes during the sensing of dopamine in the presence of UA and AA through CV studies. The determination of dopamine and its interference with UA and AA was also studied in detail by DPV technique with the detection limit of 1.03×10^{-6} mol L^{-1}. It is very clearly from this study that dopamine grafted ERG/PMB composite modified electrode towards dopamine sensing exhibits very low LOD than the PDA-

RGO/Au system. Hence, we have successfully explained that the formed ERG/PMB Grafted dopamine Composite surface as a catalytic platform for the sensing of dopamine. The selectivity of dopamine with linear range in calibration was between 0.96×10^{-6} mol L^{-1} to 7.68×10^{-6} mol L^{-1}.

ACKNOWLEDGEMENTS

Demudu Babu Gorle gratefully acknowledges UGC, New Delhi for his Research Fellowship. The authors also thank Dr. Vijayamohanan K. Pillai, Director, CSIR-CECRI for his keen interest and encouragements in our research activities. This research was financially supported by the Department of Science and Technology, New Delhi (GAP 08/13).

REFERENCES

1 H. Wang, T. Maiyalagan, X. Wang, *ACS Catal.*, 2012, **2**, 781–794.

2 T.K. Das, S. Prusty, *Polym. Technol. Eng.*, 2013, **52**, 319–331.

3 J.R. Potts, D.R. Dreyer, C.W. Bielawski, R.S. Ruoff, *Polymer*, 2011, **52**, 5–25.

4 D.A. Brownson, D.K. Kampouris, C.E. Banks, *J. Power Sources*, 2011, **196**, 4873–4885.

5 B.G. Choi, H. Park, T.J. Park, M.H. Yang, J.S. Kim, S.Y. Jang, N.S. Heo, S.Y. Lee, J. Kong, W.H. Hong, *ACS Nano*, 2010, **4**, 2910–2918.

6 Y. Zhang, T.R. Nayak, H. Hong, W. Cai, *Nanoscale*, 2012, **4**, 3833–3842.

7 P. Blake, P.D. Brimicombe, R.R. Nair, T.J. Booth, D. Jiang, F. Schedin, L.A. Ponomarenko, S.V. Morozov, H.F. Gleeson, E.W. Hill, *Nano Lett.*, 2008, **8**, 1704–1708.

8 B. Standley, A. Mendez, E. Schmidgall, M. Bockrath, *Nano Lett.*, 2012, **12**, 1165–1169.

9 G. Eda, G. Fanchini, M. Chhowalla, *Nat. Nanotechnol*., 2008, **3**, 270–274.

10 Y. Xu, C. Chen, V.V. Deshpande, F.A. DiRenno, A. Gondarenko, D.B. Heinz, S. Liu, P. Kim, J. Hone, *Appl. Phys. Lett*., 2010, 97

11 X.F. Li, L.L. Wang, K.Q. Chen, Y. Luo, *J. Phys. Chem. C*, 2011, **115**, 24366–24372.

12 A.C. Neto, F. Guinea, N.M.R. Peres, K.S. Novoselov, A.K. Geim, *Rev. Mod. Phys*., 2009, 81

13 D.S.L. Abergel, V. Apalkov, J. Berashevich, K. Ziegler, T. Chakraborty, *Adv. Phys.*, 2010, **59**, 261 -482.

14 J.W. Suk, R.D. Piner, J. An, R.S. Ruoff, *ACS Nano*, 2010, **4**, 6557–6564.

15 Yungang. Zhou, Zhiguo. Wang, Ping. Yang, Fei. Gao, *J. Phys. Chem. C*, 2012, **116**, 7581─7586.

16 A.A. Balandin, *Nat. Mater.*, 2011, **10**, 569–581.

17 S. Stankovich, D.A. Dikin, R.D. Piner, K.A. Kohlhaas, A. Kleinhammes, Y. Jia, Y. Wu, S.T. Nguyen, R.S. Ruoff, *Carbon*, 2007, **45**, 1558–1565.

18 H. Kim, A.A. Abdala, C.W. Macosko, *Macromolecules*, 2010, **43**, 6515–6530.

19 C. Macosko, *APS Meeting Abstracts*, 2010

20 S. Pei, H.M. Cheng, *Carbon,* 2012, **50**, 3210–3228.

21 D.R. Dreyer, S. Park, C.W. Bielawski, R.S. Ruoff, *Chem. Soc. Rev*., 2010, **39**, 228–240.

22 J. Liu, S. Mu, *Synth. Met.*, 1999, **107**, 159–165.

23 K. Gurunathan, A.V. Murugan, R. Marimuthu, U. Mulik, D. Amalnerkar, *Mater. Chem. Phys*., 1999, **61**, 173─191.

24 M.M. Barsan, E.M. Pinto, C. Brett, *Electrochimica Acta*, 2008, **53**, 3973–3982.

25 C. Brett, G. Inzelt, V. Kertesz, *Anal. Chim. Acta*, 1999, **385**, 119–123.

26 E. Erçarıkcı, K. Dağcı, E. Topçu, M. Alanyalıoğlu, *Mater. Res. Bull.*, 2014, **55**, 95–101.

27 M. Wojtoniszak, D. Rogińska, B. Machaliński, M. Drozdzik, E. Mijowska, *Mater. Res. Bull.*, 2013, **48**, 2636–2639.

28 D. Belanger, J. Pinson, *Chem. Soc. Rev.*, 2011, **40**, 3995–4048.

29 S.H. Hosseini, J. Simiari, B. Farhadpour, *Iran Polym J*, 2009, **18**, 3–13.

30 A. Bhattacharya, B.N. Misra, *Prog. Polym. Sci.*, 2004, **29**, 767–814.

31 J. Ghilane, F. Hauquier, J.C. Lacroix, *Anal. Chem.*, 2013, **85**, 11593–11601.

32 R. Salgado, R. del Rio, M.A. del Valle, F. Armijo, *J. Electroanal. Chem.*, 2013, **704**, 130-136.

33 W.S. Hummers, R.E. Offeman, *J. Am. Chem. Soc.,* 1958, **80**, 1339–1339.

34 Y. Zhu, S. Murali, W. Cai, X. Li, J.W. Suk, J.R. Potts, R.S. Ruoff, *Adv. Mater.*, 2010, **22**, 3906-3924.

35 Q. Liu, Y. Li, L. Zhang, D. Li, C. Fan, Y. Long, *Electroanalysis*, 2010, **22**, 2862–2870.

36 E. Topcu, M. Alanyalioglu, *Journal of Applied Polymer Science*, 2014, **131**, 39686.

37 A.A. Karyakin, E.E. Karyakin, H.L. Schmidt, *Electroanalysis*, 1999, **22**, 149-155.

38 M. Zhou, Y. Wang, Y. Zhai, J. Zhai, W. Ren, F. Wang, S. Dong, 2009, **15**, 6116-6120.

39 L. Chen, Y. Tang, K. Wang, C. Liu, S. Luo, *Electrochem. Commun.*, 2011, **13**, 133–137.

40 Y. Shao, J. Wang, M. Engelhard, C. Wang, Y. Lin, *J. Mater. Chem*., 2010, **20**, 743–748.

41 M.I.C. Marinho, M.F. Cabral, L.H. Mazo, *J. Electroanal. Chem*., 2012, **685**, 8–14.

42 G.K. Ramesha, A. Vijaya Kumara, H.B. Muralidhara, S. Sampath, *J. Colloid Interface Sci.*, 2011, **361**, 270–277.

43 H. Han, D. Pan, X. Wu, Q. Zhang, H. Zhang, *J. Mater. Sci.*, 2014, **49**, 4796–4806.

44 T. Lindfors, A. Österholm, J. Kauppila, M. Pesonen, *Electrochimica Acta*, 2013, **110**, 428–436.

45 S.T. Yang, S. Chen, Y. Chang, A. Cao, Y. Liu, H. Wang, *J. Colloid Interface Sci.*, 2011, **359**, 24–29.

46 R.A. Zangmeister, T.A. Morris, M.J. Tarlov, *Langmuir*, 2013, **29**, 8619–8628.

47 W. Lee, J.U. Lee, B.M. Jung, J.H. Byun, J.W. Yi, S. B. Lee, B.S. Kim, *Carbon*, 2013, **65**, 296-304.

48 W. Wang, A. Zhang, L. Liu, M. Tian, L. Zhang, *J. Electrochem. Soc.*, 2011, **158**, D228–D233.

49 Q. Wei, F. Zhang, J. Li, B. Li, C. Zhao, *Polym. Chem.*, 2010, **1**, 1430–1433.

50 D. Yang, A. Velamakanni, G. Bozoklu, S. Park, M. Stoller, R.D. Piner, S. Stankovich, I. Jung, D.A. Field, C.A. Ventrice Jr, *Carbon*, 2009, **47**, 145–152.

51 R. Rozada, J.I. Paredes, S. Villar-Rodil, A. Martínez-Alonso, J.M. Tascón, *Nano Res.*, 2013, **6**, 216-233.

52 J. Lv, L.S. T Sheng, G. Xu, D. Wang, Z. Zheng, *Appl. Surf. Sci.*, 2013, **284**, 229-234.

53 W. Chen, L. Yan, P.R. Bangal, *J. Phys. Chem. C*, 2010, **114**, 19885–19890.

54 G.T.S. How, A. Pandikumar, H.N. Ming, L.H. Ngee, *Scientific Reports*, 2014, **4**, 5044─5051.

55 S.K. Palanisamy, *Electrochimica Acta*, 2014, **138**, 302-310.

56 W. Sun, Y. Wang, Y. Zhang, X. Ju, G. Li, Z. Sun, *Analytica Chimica Acta,* 2012, **751**, 59-65.

57 N. Li, E. Zheng, X. Chen, S. Sun, C. You, Y. Ruan, X. Weng, *Int. J. Electrochem. Sci.*, 2013, **8**, 6524-

6534.

58 W. Wang, G. Xu, X.T. Cui, G. Sheng, X. Luo, *Biosensors and Bioelectronics*, 2014, **58**, 153-156.

59 L. Fu, G. Lai, A. Yu, *1st International Electronic conference on Materials*, McGill University, Montreal, Canada, 26 May- 10 June, 2014.

60 K.N. Kudin, B. Ozbas, H.C. Schniepp, R.K. Prud'homme, I. A. Aksay, R. Car, *Nano Lett.*, 2008, **8**, 36-41.